Evaluation of a 1,4,7,10-Tetraazacyclododecane-1,4,7,10-Tetraacetic Acid–Conjugated Bombesin-Based Radioantagonist for the Labeling with Single-Photon Emission Computed Tomography, Positron Emission Tomography, and Therapeutic Radionuclides

Rosalba Mansi,[1] Xuejuan Wang,[1] Flavio Forrer,[2] Stefan Kneifel,[2] Maria-Luisa Tamma,[1] Beatrice Waser,[3] Renzo Cescato,[3] Jean Claude Reubi,[3] and Helmut R. Maecke[1]

Abstract

Purpose: G protein–coupled receptor agonists are being used as radiolabeled vectors for *in vivo* localization and therapy of tumors. Recently, somatostatin-based antagonists were shown to be superior to agonists. Here, we compare the new [^{111}In/^{68}Ga]-labeled bombesin-based antagonist RM1 with the agonist [^{111}In]-AMBA for targeting the gastrin-releasing peptide receptor (GRPR).

Experimental Design: IC_{50}, K_d values, and antagonist potency were determined using PC-3 and HEK-GRPR cells. Biodistribution and imaging studies were done in nude mice transplanted with the PC-3 tumor. The antagonist potency was assessed by evaluating the effects on calcium release and on receptor internalization monitored by immunofluorescence microscopy.

Results: The IC_{50} value of [^{nat}In]-RM1 was 14 ± 3.4 nmol/L. [$^{nat/111}$In]-RM1 was found to bind to the GRPR with a K_d of 8.5 ± 2.7 nmol/L compared with a K_d of 0.6 ± 0.3 nmol/L of [^{111}In]-AMBA. A higher maximum number of binding site value was observed for [^{111}In]-RM1 (2.4 ± 0.2 nmol/L) compared with [^{111}In]-AMBA (0.7 ± 0.1 nmol/L). [^{nat}Lu]-AMBA is a potent agonist in the immunofluorescence-based internalization assay, whereas [^{nat}In]-RM1 is inactive alone but efficiently antagonizes the bombesin effect. These data are confirmed by the calcium release assay. The pharmacokinetics showed a superiority of the radioantagonist with regard to the high tumor uptake (13.4 ± 0.8% IA/g versus 3.69 ± 0.75% IA/g at 4 hours after injection. as well as to all tumor-to-normal tissue ratios.

Conclusion: Despite their relatively low GRPR affinity, the antagonists [^{111}In/^{68}Ga]-RM1 showed superior targeting properties compared with [^{111}In]-AMBA. As found for somatostatin receptor–targeting radiopeptides, GRP-based radioantagonists seem to be superior to radioagonists for *in vivo* imaging and potentially also for targeted radiotherapy of GRPR-positive tumors. (Clin Cancer Res 2009;15(16):5240–9)

Peptide receptors are promising targets for molecular imaging and targeted radionuclide therapy of cancer (1–3). Somatostatin receptors are prototypic and were successfully targeted with radiolabeled peptides for diagnostic imaging (4) and therapeutic application (5). Radiolabeled agonists were developed because they usually trigger the internalization of the radiopeptide-receptor complex, an important mechanism for active uptake and accumulation of the radiopeptides considered to be crucial for efficient targeting and residence of the radiotracer in the tumor.

We have recently shown that somatostatin-based radiolabeled antagonists may have a higher and longer lasting tumor uptake than equipotent agonists (6). This may represent a shift in paradigm, if proven for other (GPCRs) G-protein coupled receptor.

Among the most promising receptors for tumor targeting are bombesin receptors as they are overexpressed in major human tumors such as prostate (7, 8), breast (9, 10), and gastrointestinal stromal tumors (11). Bombesin receptors mediate different physiologic responses and are involved in cancerogenesis. Experimental findings indicate that bombesin-like peptides may act as autocrine growth factors on (SCLC) small cell lung cancer and other cancer types (12, 13). Therefore gastrin-releasing peptide receptor (GRPR) antagonists were developed as targeted anticancer agents. They show antitumor activity in murine and

Authors' Affiliations: [1]Division of Radiological Chemistry and [2]Institute of Nuclear Medicine, University Hospital Basel, Basel, Switzerland; and [3]Division of Cell Biology and Experimental Cancer Research, Institute of Pathology, University of Berne, Berne, Switzerland

Received 12/5/08; revised 5/14/09; accepted 5/14/09; published OnlineFirst 8/11/09.

Grant support: Swiss Cancer League (grant number OCS-01778-08-2005 and the Swiss National Science Foundation (grant number 320000-118333). The costs of publication of this article were defrayed in part by the payment of page charges. This article must therefore be hereby marked *advertisement* in accordance with 18 U.S.C. Section 1734 solely to indicate this fact.

Note: Supplementary data for this article are available at Clinical Cancer Research Online (http://clincancerres.aacrjournals.org/).

Requests for reprints: Helmut R. Maecke, Division of Radiological Chemistry, University Hospital Basel, Petersgraben 4, CH-4031 Basel, Switzerland. Phone: 41-61-265-46-99; Fax: 41-61-265-55-59; E-mail: hmaecke@uhbs.ch.

doi:10.1158/1078-0432.CCR-08-3145

Translational Relevance

Prostate cancer is one of the most frequent cancers in men. New imaging methods delineating the tumor and determining the spread of disease, in particular to the bone, are needed. A highly and frequently overexpressed tumor cell surface marker of prostate cancer cells is the gastrin-releasing peptide receptor. Clinical studies with radiolabeled bombesin-based agonists showed promising results. In this article, we compare one of the most potent agonists ([^{111}In]-AMBA) with a 1,4,7,10-tetraazacyclododecane-1,4,7,10-tetraacetic acid–conjugated antagonist ([^{111}In]-, [^{68}Ga]-RM1) for imaging and potentially targeted radionuclide therapy. Pharmacokinetic studies showed a distinct advantage of radiolabeled RM1 over the agonist with regard to tumor uptake and tumor-to-normal tissue ratios. Therefore, the new radiopeptide is an excellent candidate for clinical studies, which we will perform in due course.

human tumors (14–16). Moreover, the development of radiolabeled peptides for imaging and targeted radionuclide therapy has been advanced in recent years (17–24). Clinical studies with [^{99m}Tc]- and [^{68}Ga]-labeled bombesin-based peptides have been reported for imaging metastasized prostate, breast, and gastrointestinal stromal tumors (25–27).

One of the most potent radiolabeled agonists described in the literature, [^{177}Lu]-DO3A-CH_2CO-G-4-aminobenzoyl-Q-W-A-V-G-H-L-M-NH_2[4] ([^{177}Lu]-AMBA), was proposed to be suitable for imaging and treatment (18) and is being studied in phase 1 clinical trials (28, 29). Several classes of bombesin antagonists have been explored by the modification of the COOH-terminal residues of amidated bombesin agonists (30). A [^{99m}Tc]-labeled antagonist based on a tetraamine ligand was recently published for potential imaging of GRPR-positive tumors (31). Compared with an agonist, it showed superior tumor uptake.

A potent bombesin receptor antagonist (H-D-Phe-Gln-Trp-Ala-Val-Gly-His-Sta-Leu-NH_2) was obtained by replacing Leu-13 with a statyl residue (32). The aim of the present study was to develop a conjugate that can be labeled with radiometals useful for single-photon emission computed tomography (SPECT) (^{111}In, ^{67}Ga), positron emission tomography (PET) (^{68}Ga, ^{86}Y), and targeted radionuclide therapy (^{90}Y, ^{177}Lu, ^{213}Bi). We report on a direct comparison of two peptides having 1,4,7,10-tetraazacyclododecane-1,4,7,10-tetraacetic acid (DOTA) as chelator and glycine-4-aminobenzoyl as spacer linking the chelate to the peptides (Fig. 1). We determined the binding affinity to GRPR of [^{nat}In]-RM1 and [^{nat}Lu]-AMBA; furthermore, the internalization, cellular, and receptor retention of the ^{111}In-labeled peptides, as well as their agonist/antagonist properties were studied. Finally, we studied the pharmacokinetics of the two peptides in the same tumor model under identical experimental conditions and did SPECT/computed tomography (CT) and PET/CT studies with [^{111}In]-RM1 and [^{68}Ga]-RM1.

[4] Abbreviations of the common amino acids are in accordance with the recommendations of IUPAC-IUB (http://www.chem.qmul.ac.uk/iupac/AminoAcid/).

Materials and Methods

All reagents were obtained from commercial sources and used without further purification. Rink amide 4-methyl-benzhydrylalanine resin and all amino acids or peptides are available from NovaBiochem or NeoMPS. DOTA-tris(^{t}Bu ester) was purchased from CheMatech. [^{111}In]Cl_3 was purchased from Covidien Medical. BIM26226 was provided by Ipsen Biotech. Electrospray ionization mass spectroscopy was carried out with a Finnigan SSQ-7000-spectrometer. Analytic high-performance liquid chromatography (RP-HPLC) was done on a Hewlett Packard 1050-HPLC-system with a multiwavelength detector and a flow-through Berthold LB-506-Cl γ-detector using a Macherey-Nagel Nucleosil 120 C_{18}-column (eluents: A, 0.1% (TFA) trifluoroacetic acid in water; and B, acetonitrile; gradient, 0-30 min, 95-30% A; flow, 0.750 mL/min). Preparative RP-HPLC was done on a Metrohm HPLC-system LC-CaDI 22-14 with a Macherey-Nagel VP 250/21 Nucleosil 100-5 C_{18}-column (gradient, 0-20 min, 90-50% A; flow, 10 mL/min). Quantitative γ-counting was done on a COBRA 5003 γ-system well counter from Packard Instruments (Packard).

Cell lines. Human embryonic kidney 293 (HEK293) cells, stably expressing the HA-epitope–tagged human GRPR (HEK-GRPR), were generated as previously described (31) and cultured at 37°C/5% CO_2 in DMEM with GlutaMAX-I containing 10% (v/v) fetal bovine serum, 100 U/mL penicillin, 100 μg/mL streptomycin, and 750 μg/mL G418. Human prostate cancer cells (PC-3) were obtained from American Type Culture Collection; cultured at 37°C and 5% CO_2 either in Ham's F12K or in DMEM containing 2 mmol/L L-glutamine and supplemented with 10% (v/v) fetal bovine serum, 100 U/mL penicillin, and 100 μg/mL streptomycin. All culture reagents were from Invitrogen or BioConcept.

Synthesis of conjugated peptides and metallation. The peptide-chelator conjugates RM1 and AMBA (Fig. 1) were synthesized manually according to standard Fmoc chemistry (33) using Rink amide 4-methyl-benzhydrylalanine resin. The spacers and the prochelator DOTA-tris(^{t}Bu ester) were consecutively coupled to the peptide. The cleavage of the peptide and simultaneous deprotection of the side chain-protecting groups were done using TFA/TA/H_2O/TIS (95/1/1/2). Purification of the peptide conjugates and metallated conjugates was according to Heppeler et al. (34), and analysis was by RP-HPLC and electrospray-mass spectrometry. The metallated peptide [^{nat}In]-RM1 and [^{nat}Lu]-AMBA were obtained as white powder in 80% yield.

Preparation of the radiotracers. The [^{111}In]-DOTA-peptide conjugates were prepared by dissolving 10 μg peptide in 250 μL sodium acetate buffer [0.4 mol/L (pH 5.0)], followed by incubation with [^{111}In]Cl_3 (100-180 MBq) for 30 min at 95°C. One equivalent of $InCl_3 \cdot 5H_2O$ was added and the final solution incubated again at 95°C for 30 min to obtain structurally characterized homogeneous ligands. For biodistribution and serum stability studies, the labeling was done without adding In-salt and the radiotracers were used without further purification. For injection, the radioligand was diluted with 0.9% NaCl (0.1% bovine serum albumin).

[^{68}Ga] was eluted and purified from a commercially available generator according to Zhernosekov et al. (35). Purified [^{68}Ga(III)] was eluted from a 50W-X8 cation exchanger chromatographic column (Bio-Rad; <400 mesh) with 400 μL 97.6% acetone/0.05 N HCl solution. This fraction (100-150 MBq) was used directly for the labeling of RM1 (20 μg) in 0.25 mol/L HEPES solution (400 μL) at pH 3.6 to 3.9 using microwave (Biotage) heating for 5 min at 95°C.

Binding affinity measurements. IC_{50} values were determined by *in vitro* GRPR autoradiography on cryostat sections of well-characterized prostate carcinomas, as described previously (7, 36). The radioligand used was [^{125}I-Tyr^4]-bombesin, known to preferentially label GRPRs (37).

Binding saturation experiments were done using increasing concentrations of [$^{111/nat}$In]-DOTA-peptides ranging from 0.1 to 1,000 nmol/L, in triplicates for both total and nonspecific binding. A 1,000-fold excess

of cold ligand ([Tyr^4]-bombesin for AMBA and BIM26226 for RM1) was used to determine nonspecific internalization. The plates were placed on ice for 30 min; then the blocking agents and radioligands were added and the plates incubated for 2 h at 4°C. Afterwards, the binding buffer was aspirated and the cells were washed twice with ice-cold PBS (pH 7.4), representing the free fraction. The cells were then collected with 1 N NaOH; this corresponded to the bound fraction. Specific binding was calculated by subtracting nonspecific from total binding at each radioligand concentration.

The affinity (K_d) and binding site density (B_{max}) were calculated from Scatchard plots using Origin 7.5 software (Microcal Software, Inc.).

Internalization studies. PC-3 cells were seeded into six-well plates overnight ($0.8\text{-}1.0 \cdot 10^6$ cells per well). On the day of the experiment, the medium was removed, the cells were washed twice with fresh medium [DMEM, 1% fetal bovine serum (pH 7.4)] and incubated for 1 h at 37°C. Approximately 3 kBq of [$^{111/nat}$In]-labeled peptide (0.25 pmol) was added to the medium and the cells were incubated (in triplicates) for 0.5, 1, 2, and 4 h at 37°C, 5% CO_2. A 1,000-fold excess of each blocking agent was used to determine nonspecific internalization. At each time point, the cells were treated exactly as described recently (24).

***The fate of GRPR-bound radiopeptides* in vitro.** PC-3 cells were seeded into six-well plates and treated as described above. The plates were placed on ice for 30 min; an excess of blocking agent was added to selected wells to determine nonspecific binding. The radioligands (0.25 pmol, 3 kBq) were added to the medium and allowed to bind to the cells for 2 h at 4°C. After the incubation, the cells were quickly washed twice with ice-cold PBS and 1 mL of fresh prewarmed (37°C) culture medium was added to each well followed by incubation for 10, 20, and 30 min and 1, 2, and 4 h (37°C, 5% CO_2). At each time point, the plates were treated as above.

Immunofluorescence microscopy. Immunofluorescence microscopy–based internalization assays with HEK-GRPR cells were done as previously described (31). HEK-GRPR cells were treated either with 10 nmol/L bombesin, or with 1 μmol/L RM26 (32), [^{nat}In]-RM1, and [^{nat}Lu]-AMBA or, to evaluate potential antagonism, with 10 nmol/L bombesin in the presence of a 100-fold excess RM26, [^{nat}In]-RM1, and [^{nat}Lu]-AMBA for 30 min at 37°C, 5% CO_2 in growth medium, and then processed for immunofluorescence microscopy using the mouse monoclonal HA-epitope antibody at a dilution of 1:1,000 as first antibody (Covance) and Alexa Fluor 488 goat anti-mouse IgG (H+L) at a dilution of 1:600 as secondary antibody (Molecular Probes). The cells were imaged using a Leica DM RB immunofluorescence microscope and an Olympus DP10 camera.

Calcium release assay. Intracellular calcium release was measured in PC-3 cells using the Fluo-4NW Calcium Assay kit (Molecular Probes) as described previously (31). In brief, PC-3 cells were seeded (10,000 cells per well) in 96-well plates and cultured for 2 d at 37°C and 5% CO_2 in culture medium. At the day of the experiment, the cells were washed with assay buffer (1× HBSS, 20 mmol/L HEPES) containing 2.5 mmol/L probenecid, and then loaded with 100 μL/well Fluo-4NW dye in assay buffer containing 2.5 mmol/L probenecid for 30 min at 37°C and 5% CO_2 and for further 30 min at room temperature. The dye-loaded cells were transferred to a SpectraMax M2^e (Molecular Devices) and, after stimulation, the intracellular calcium release was recorded for 60 s at room temperature monitoring fluorescence emission at 520 nm (λ_{ex} = 485 nm) in the presence of the analogues at the indicated concentrations. Maximum fluorescence was measured after addition of 25 μmol/L ionomycin (31, 38).

Biodistribution in PC-3 tumor–bearing nude mice. All animal experiments were done in compliance with the Swiss regulations (permit #789).

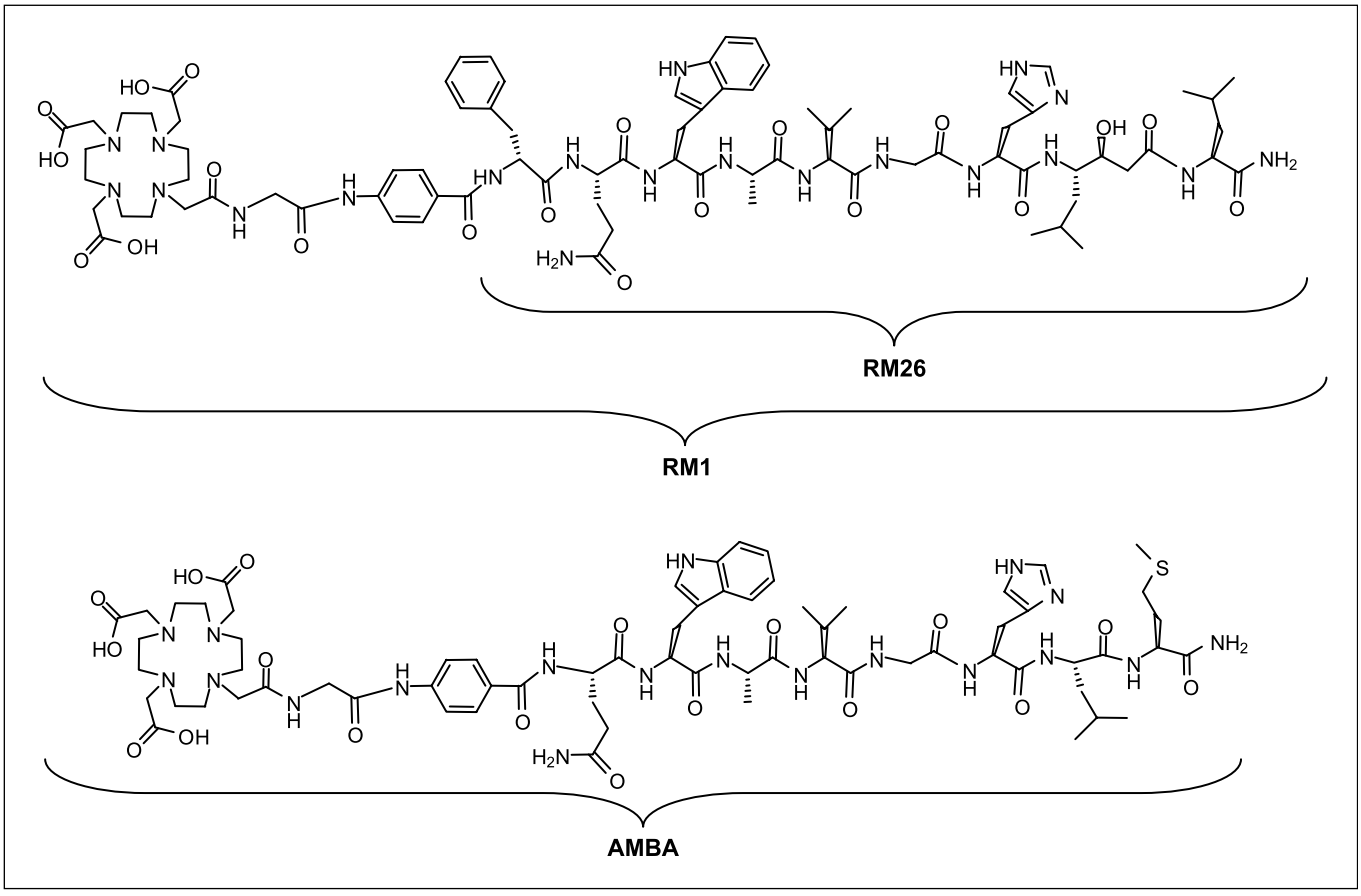

Fig. 1. Structural formulae of RM1, RM26 (32), and AMBA.

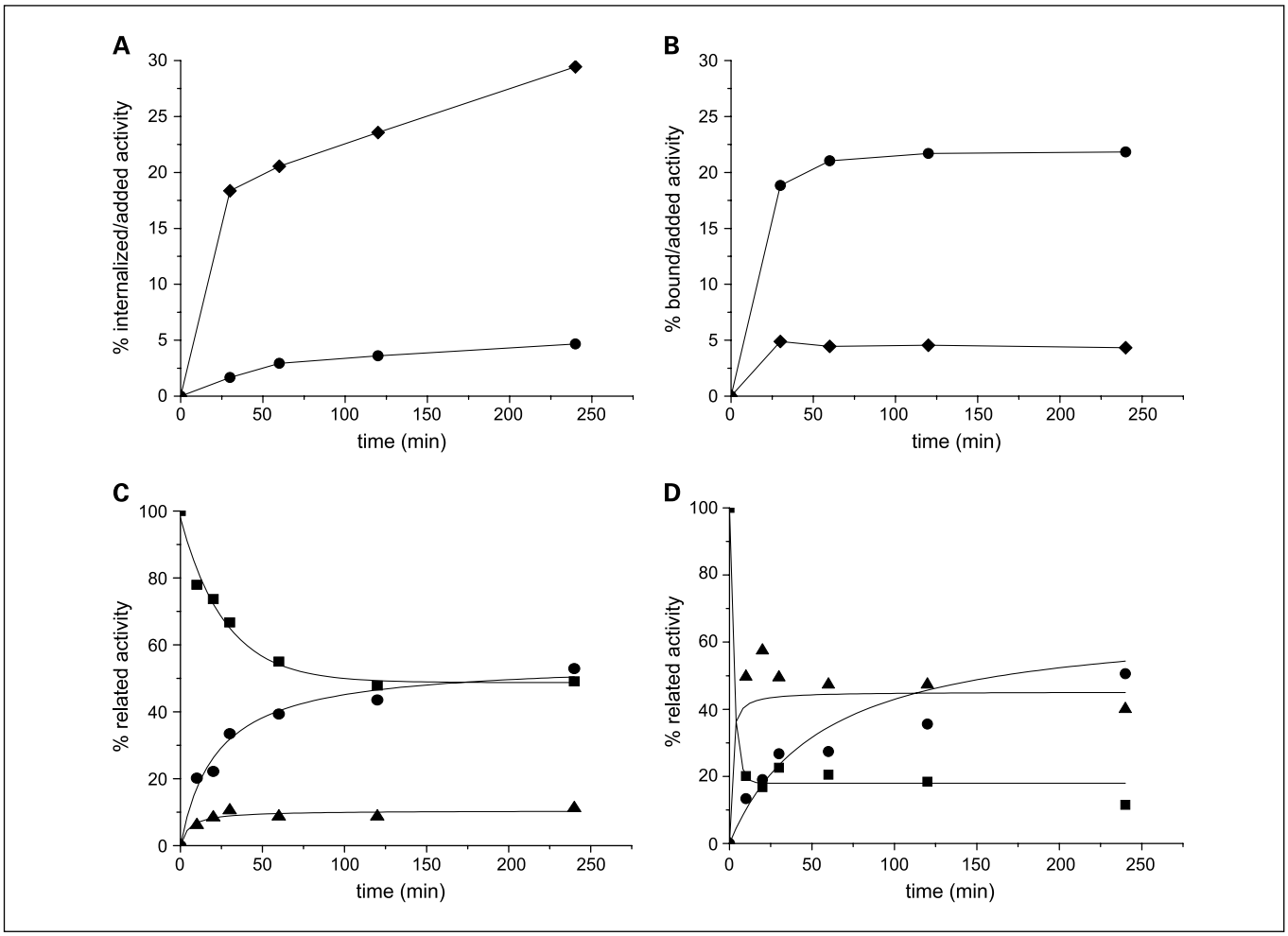

Fig. 2. Internalization of [^{111}In]-RM1 (●) was found significantly lower compared with [^{111}In]-AMBA (♦) in PC-3 cells (*A*). Conversely, higher percent of [^{111}In]-RM1 (●) remained bound to the cell membrane of PC-3 cells in comparison with [^{111}In]-AMBA (♦; *B*). The fate of the GRPR-bound [^{111}In]-RM1 (*C*) and [^{111}In]-AMBA (*D*). At the specified times, the amount of radioactivity present as free (●), surface-bound (■), and internalized (▲) ligand was determined as described in Materials and Methods. Each time point is the average of triplicate wells corrected for nonspecific binding.

Female nude mice were implanted s.c. with 10 million PC-3 tumor cells, which were freshly expanded in sterilized PBS (pH 7.4). Eleven days after inoculation, the tumors grew to a size of 5 ± 2 mm. The mice were injected into the tail vein with 10 pmol of ^{111}In-radiolabeled peptides (about 0.18 MBq, 100 μL). For the determination of nonspecific uptake in the tumor or receptor-positive organs, a group of four animals was preinjected (5 min) with 20 nmol of unlabeled peptide. Mice were sacrificed at 1, 4, 24, 48, and 72 h, and the organs of interest were collected, rinsed of excess blood, weighed, and counted in a γ-counter. The percentage of injected activity per gram (% IA/g) was calculated for each tissue.

For biodistribution studies of [^{68}Ga]-RM1, mice were sacrificed at 1 and 2 h after injection.

In vivo ***radioligand displacement using excess of cold peptide.*** Mice were injected with 10 pmol of [^{111}In]-RM1 (0.18 MBq, 100 μL), as described above, to study if the radioligand can be displaced *in vivo* by excess of cold peptide. Twenty nanomoles of cold peptide (100 μL saline) were injected at 1, 4, and 24 h, and mice were sacrificed 1 h after injection.

Influence of RM1 mass on pharmacokinetics of [^{111}In]-RM1. Receptor saturation experiments were done at four different concentrations of [^{111}In]-RM1 (10, 50, 100, 250 pmol/100 μL, 0.18 MBq) and two time points (4 and 24 h).

Biodistribution when receptors were preoccupied by cold antagonist. Twenty nanomoles of RM1 (100 μL) were preinjected, and after 1, 4, and 24 h, [^{111}In]-RM1 (10 pmol, 100 μL) was injected for receptor occupancy studies and the mice were sacrificed 1 h after administration.

SPECT/CT imaging of [^{111}In]-RM1. PC-3 tumor–bearing nude mice were injected with 4 MBq of [^{111}In]-RM1 (100 pmol). Twenty nanomoles RM1 were preinjected for blocking studies. Images were acquired at 4, 24, 48, and 72 h after injection using a clinical SPECT/CT camera (Symbia T2). Iteratively reconstructed SPECT images (four subsets, eight iterations) were fused with three-dimensional reconstructed images from the CT (2 × 1.25 mm slices, 130 kV, 48 mAs).

PET/CT imaging of [^{68}Ga]-RM1. PC-3 tumor–bearing nude mice were sacrificed 1 h after injection of 0.5 MBq [^{68}Ga]-RM1 (100 pmol) and images were acquired using a clinical PET/CT scanner (Discovery STE, GE Medical Systems). PET emission events were collected in three-dimensional scanning mode (septa out) over 60 min. The acquired data were corrected for [^{68}Ga] decay and random events and reconstructed using the manufacturer's 3D-OSEM algorithm. The images were fused with three-dimensional reconstructed images from the CT (16 × 0.625 mm slices, 120 KeV, 320 mA).

Statistical analysis. Data are expressed as mean ± SD, calculated on Microsoft Excel. Origin 7.5 software (Microcal Software, Inc.) was used to determine statistical significance at the 95% confidence level with a P value of <0.05 being considered significantly different.

Results

Chemistry; radiochemistry. The peptide-chelator conjugates were obtained with a yield of ~30% and were characterized

by electrospray-mass spectrometry (RM1, 1715.1 [M+K$^+$]; [^{nat}In]-RM1, 1788.9 [M+H$^+$]; AMBA, 1541.4 [M+K$^+$]; [^{nat}Lu]-AMBA, 1675.8 [M+H$^+$]); their purity was assessed by RP-HPLC. [^{68}Ga]-labeling was done using microwave heating (5 minutes, 95°C) with labeling yields of ≥95% at a specific activity of 18 GBq μmol^{-1}. [^{111}In]-labeled conjugates were obtained by incubation at elevated temperature (95°C, 30 minutes) with labeling yields of ≥95% at a maximum specific activity of 30 GBq μmol^{-1}.

Binding affinity measurements. The IC_{50} values of the peptides showed that compared with the reference peptide RM26 (IC_{50}, 5.6 ± 1.8 nmol/L), RM1, and [^{nat}In]-RM1 still retained reasonable affinity to the GRPR (IC_{50}, 35 ± 13 nmol/L and 14 ± 3.4 nmol/L, respectively). The IC_{50} value of [^{nat}Lu]-AMBA was 0.8 ± 0.1 nmol/L. The K_d values of [$^{nat/111}$In]-RM1 and [$^{nat/111}$In]-AMBA are 8.5 ± 2.7 nmol/L and 0.6 ± 0.3 nmol/L at 4°C, respectively. A higher B_{max} value was observed for [^{111}In]-RM1 (2.4 ± 0.2 nmol/L) compared with [^{111}In]-AMBA (0.7 ± 0.1 nmol/L).

Internalization studies. [^{111}In]-RM1 and [^{111}In]-AMBA showed specific and time-dependent cell uptake (at 37°C). At 4 hours, the internalized activity was 4.66 ± 0.08% for [^{111}In]-RM1; 21.8 ± 0.93% was surface-bound. The internalized activity of [^{111}In]-AMBA was 29 ± 2.3%, whereas the surface-bound activity was 4.33 ± 0.27% at 4 hours (Fig. 2A and B).

The fate of GRPR-bound radiopeptides. The fate of the receptor-bound radiopeptides was studied by a temperature shift experiment; the two radiopeptides showed a distinct difference (Fig. 2C and D). At 4 hours, 40% of [^{111}In]-AMBA was internalized and 50% was found dissociated with an approximate half-life of 1 hour (D), whereas for [^{111}In]-RM1, the amount of ligand dissociating from the cells at 37°C was 50% of the total ligand prebound. Only ~10% of the surface-bound ligand was internalized within 30 min, whereas the rest was still bound to the receptors (C).

Immunofluorescence microscopy. The agonist and antagonist properties of the bombesin analogues were confirmed by immunofluorescence-based internalization assay using HEK-GRPR cells. Figure 3A illustrates that 10 nmol/L bombesin can trigger internalization of the receptors. [^{nat}Lu]-AMBA at 1,000 nmol/L also induces internalization of GRPRs, whereas [^{nat}In]-RM1 and RM26 were not able to stimulate GRPR internalization. However, when given at a concentration of 1,000 nmol/L together with 10 nmol/L bombesin, both peptides are able to prevent bombesin-induced receptor internalization.

Calcium release. The calcium release assay was done to determine dose-response curves of the bombesin antagonists in PC-3 cells. As seen in Fig. 3B, bombesin alone can stimulate calcium release. RM1, [^{nat}In]-RM1, and RM26 behave like antagonists shifting the dose-response curve of bombesin to a higher molar range when given at 10 μmol/L together with bombesin. The dose-response curve is shifted to higher bombesin concentrations corresponding to the lower IC_{50} values. Moreover, tested alone at 1 and 10 μmol/L, the three peptides have no effect on calcium release.

Biodistribution studies. [^{111}In]-RM1 and [^{111}In]-AMBA pharmacokinetics are characterized by a fast blood clearance, 0.04% IA/g for [^{111}In]-RM1, and 0.05% IA/g for [^{111}In]-AMBA remaining in blood at 4 hours after injection. (Table 1).

The tumor uptake at 1 hour was 14.2 ± 1.75% IA/g for [^{111}In]-RM1 and 4.48 ± 0.68% IA/g for [^{111}In]-AMBA. Both radiopeptides showed little washout at 4 hours after injection.

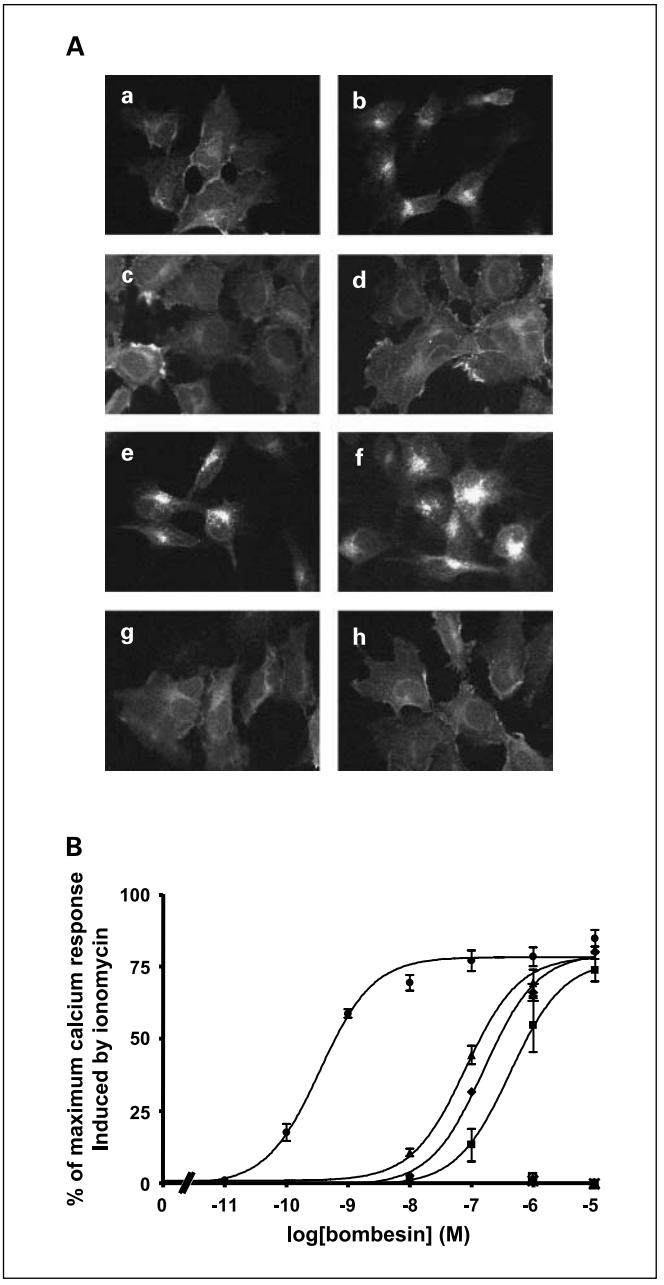

Fig. 3. *A,* GRPR internalization induced by bombesin is efficiently antagonized by the bombesin analogues RM26 and [^{nat}In]-RM1 but not by the agonist [^{nat}Lu]-AMBA. HEK-GRPR cells were treated for 30 min either with vehicle (no peptide, *a*), or with 10 nmol/L bombesin (*b*), a concentration inducing a submaximal internalization effect. *d, f,* and *h,* cells treated with 10 nmol/L bombesin in the presence of 1 μmol/L of the analogues RM26 (*d*), [^{nat}Lu]-AMBA (*f*), and [^{nat}In]-RM1 (*h*). *c, e,* and *g,* the effect of RM26 (*c*), [^{nat}Lu]-AMBA (*e*), and [^{nat}In]-RM1 (*g*) when given alone at a concentration of 1 μmol/L. Following incubation with the peptides, the cells were processed for immunofluorescence microscopy as described in Materials and Methods. *B,* dose-response curves of bombesin analogues determined by the calcium release assay as described in Materials and Methods. PC-3 cells were treated either with bombesin at concentrations ranging between 0.01 nmol/L and 10 μmol/L (●) alone, or with bombesin at concentrations ranging between 10 nmol/L and 10 μmol/L in the presence of 10 μmol/L of the analogues RM1 (▲), or [^{nat}In]-RM1 (♦), or the bombesin antagonist RM26 (■). RM1, [^{nat}In]-RM1, and RM26 behave like antagonists shifting the dose-response curve of bombesin to a higher molar range. Tested alone at 1 and 10 μmol/L RM1 (△), [^{nat}In]-RM1 (×) and RM26 (□) have no effect on calcium release in PC-3 cells. Data are expressed as percentage of maximum calcium response induced by ionomycin.

Table 1. Biodistribution studies in PC-3 tumor–bearing mice at 1, 4, and 24 h (n = 3-4 mice per time point) after injection of [^{111}In]-RM1 and [^{111}In]-AMBA and tumor to tissue radioactivity ratios

Organ	Time (h)	[^{111}In]-RM1 (%ID/g tissue ± SD)		[^{111}In]-AMBA (%ID/g tissue ± SD)	
		Nonblocked	Blocked*	Nonblocked	Blocked*
Blood	1	0.86 ± 0.17		0.33 ± 0.03	
	4	0.04 ± 0.00	0.02 ± 0.01	0.05 ± 0.00	0.05 ± 0.01
	24	0.01 ± 0.00		0.02 ± 0.01	
Tumor	1	14.24 ± 1.75		4.48 ± 0.68	
	4	13.46 ± 0.80	0.46 ± 0.00	3.69 ± 0.75	0.44 ± 0.03
	24	6.58 ± 1.14		2.95 ± 0.55	
Kidneys	1	3.99 ± 0.33		3.98 ± 0.86	
	4	1.93 ± 0.18	2.67 ± 0.10	2.31 ± 0.60	1.58 ± 0.31
	24	1.01 ± 0.06		1.29 ± 0.08	
Pancreas	1	21.92 ± 1.34		59.95 ± 6.15	
	4	1.32 ± 0.31	0.07 ± 0.02	49.44 ± 3.27	0.29 ± 0.06
	24	0.15 ± 0.02		47.11 ± 0.86	
Muscle	1	0.19 ± 0.06		0.17 ± 0.01	
	4	0.03 ± 0.01	0.02 ± 0.00	0.10 ± 0.02	0.06 ± 0.07
	24	0.03 ± 0.00		0.14 ± 0.01	
Intestine	1	1.73 ± 0.48		4.09 ± 0.27	
	4	0.20 ± 0.10	0.07 ± 0.01	2.68 ± 0.29	0.14 ± 0.03
	24	0.04 ± 0.00		1.79 ± 0.15	
Liver	1	1.93 ± 0.29		0.26 ± 0.02	
	4	0.38 ± 0.05	0.39 ± 0.08	0.16 ± 0.02	0.25 ± 0.04
	24	0.19 ± 0.01		0.14 ± 0.01	
Stomach	1	3.31 ± 0.63		3.27 ± 0.45	
	4	0.76 ± 0.14	0.07 ± 0.03	2.42 ± 0.08	0.08 ± 0.01
	24	0.05 ± 0.02		1.95 ± 0.24	
Lung	1	0.82 ± 0.13		0.38 ± 0.03	
	4	0.12 ± 0.04	0.10 ± 0.03	0.14 ± 0.02	0.08 ± 0.01
	24	0.05 ± 0.01		0.14 ± 0.01	
Bone	1	0.40 ± 0.10		0.40 ± 0.07	
	4	0.18 ± 0.07	0.04 ± 0.01	0.31 ± 0.05	0.07 ± 0.01
	24	0.14 ± 0.03		0.24 ± 0.07	

Tumor-to-tissue ratios	[^{111}In]-RM1 (1/4/24 h after injection)	[^{111}In]-AMBA (1/4/24 h after injection)
Tumor/blood	16.6/336/658	13.6/74/147
Tumor/kidneys	3.6/7.0/6.5	1.1/1.6/2.3
Tumor/muscle	75/448/219	26.3/36.9/21.1
Tumor/liver	7.4/35.4/34.6	17.2/23.1/21.1
Tumor/intestine	8.2/67.3/164.5	1.1/1.4/1.6

*Blocked witd 20 nmoles of the corresponding DOTA peptides.

(13.46 ± 0.8% IA/g and 3.69 ± 0.75% IA/g, respectively). Tumor uptake was specific as shown by preinjection of 2,000 times excess of the respective cold peptides. At 4 hours, 96.6% blocking was shown for [^{111}In]-RM1 and 88.1% for [^{111}In]-AMBA. The tumor uptake of both radiopeptides stays high also at 24 hours. Due to the rapid clearance, particularly of [^{111}In]-RM1, from nonspecifically targeted organs, very high tumor-to-background ratios were found that increased with time; the tumor-to-blood ratios for [^{111}In]-RM1 (in brackets, the values for [^{111}In]-AMBA) increased from 16.5 (13.6) at 1 hour to 336.5 (73.8) at 4 hours, 658 (147.5) at 24 hours, 1,600 at 48 hours, and 1871 at 72 hours (see Supplementary Data). The uptake in the GRPR-expressing organs pancreas, stomach, and intestines was high and specific for both radiopeptides, but [^{111}In]-RM1 was washed out very quickly compared with [^{111}In]-AMBA. The kidney uptake was low for both radiopeptides.

The pharmacokinetic data presented here for [^{111}In]-AMBA correlate well with data recently reported in an abstract by J. Fox et al. (39), except for the pancreas.

[^{68}Ga]-RM1 also showed very favorable pharmacokinetics (see supplementary). The tumor uptake was similar to that of [^{111}In]-RM1 whereas the kidney uptake was significantly lower at 1 h (2.85 ± 0.39% IA/g for [^{68}Ga]-RM1 and 3.99 ± 0.33% IA/g for [^{111}In]-RM1). The washout from the kidneys is faster for [^{68}Ga]-RM1 (1.28 ± 0.11% IA/g at 2 h) compared with [^{111}In]-RM1 (1.93 ± 0.18% IA/g at 4 h).

Radioligand displacement using excess of cold peptide. We studied if the radioligands can be displaced by 2,000-fold excess of RM1 at 1, 4, and 24 hours after injection. The data of selected GRPR-positive organs and the tumor are shown in Table 2A. At 1 hour, 89% of the radioligand can be displaced from the tumor; at 4 hours, it is still 84%, and at 24 hours, 58%. Similar results were obtained for other GRPR-positive organs at 1 hour. No significant

differences were found in receptor-negative organs. The same experiment with [^{111}In]-AMBA indicated that at 1 hour, there is no displacement. This is in agreement with the assumption that the radioagonist is already internalized *in vivo* at early time points.

Influence of cold RM1 on the pharmacokinetics of [^{111}In]-RM1. Table 2B shows the influence of the peptide mass on the pharmacokinetics. Our control protocol foresees the use of 0.18 MBq [^{111}In]-RM1(10 pmol), which corresponds to an 80-fold excess of RM1 over [^{111}In]. We studied how the increase of RM1 influences the pharmacokinetics, in particular uptake and retention in tumor and receptor-positive tissues. A 5-fold RM1 increase has no significant influence on the tumor uptake ($P < 0.05$) at 4 hours, whereas a 10- and 25-fold excess lowers it significantly by about 20% to 40%, indicating the onset of receptor saturation in the tumor. The influence of the peptide mass to saturate GRPR-binding sites in the stomach, intestines and pancreas is more significant. The higher peptide mass also seems to increase the washout rate from these tissues but does not seem to have an influence on the retention time in the tumor.

Receptor occupancy by cold peptide. Given that [^{111}In]-RM1, a full antagonist, is not being internalized *in vivo*, the retention time in the tumor is unexpectedly long (Table 2C). We designed an experiment injecting large excess of RM1 (2,000-fold) leading to 96.6% tumor receptor uptake blocking in the control experiment. We allowed 1, 4, and 24 hours before injecting [^{111}In]-RM1 and an additional hour before sacrificing the animals to perform biodistribution studies. Compared with the 1-hour data, the tumor uptake was partially blocked by pretreatment with RM1. About 70% of the receptors are blocked by the preinjected excess of cold peptide at 1 hour, still ~38% at 4 hours, and ~17% at 24 hours, compared with the control. A significant decrease in pancreatic uptake was seen at each time point (87% at 1 hour; 17% at 4 hours and 3% at 24 hours). The excess of cold peptide was released faster from these organs than from the tumor. In the same experiment, the radioagonist uptake was fully restored 2 hours after excess agonist injection (data not shown), indicating full receptor availability for radioagonist binding.

Imaging studies. Figure 4A (*a*, *e*, *f*, and *g*) shows the coronal SPECT/CT scans 4, 24, 48, and 72 hours after injection of 4 MBq [^{111}In]-RM1 (100 pmols peptide). Figure 4Ab is the image obtained after 5 min preinjection of 20 nmoles RM1. The transaxial SPECT/CT images at 4 hours after injection (unblocked/blocked) in Fig. 4Ac and Ad show high, specific tumor uptake and fast washout from GRPR-positive organs, depending on the higher peptide mass injected, reflecting the mass dependence on pharmacokinetics (Table 2B).

Table 2. Mechanistic pharmacokinetic studies

A. Radioligand displacement of [^{111}In]-RM1 in selected GRPR-positive tissues and the PC-3 tumor at different time points (1, 4, 24 h)

Organ	1 h	1 h displ.	4 h	4 h displ.	24 h	24 h displ.
Tumor	14.24 ± 1.75	1.59 ± 0.9	13.46 ± 0.80	2.20 ± 0.36	6.58 ± 1.14	2.79 ± 0.4
Pancreas	21.9 ± 1.34	0.55 ± 0.04	1.32 ± 0.31	0.49 ± 0.04	0.15 ± 0.02	0.07 ± 0.01
Stomach	3.3 ± 0.63	0.18 ± 0.02	0.76 ± 0.14	0.33 ± 0.4	0.05 ± 0.02	0.05 ± 0.02
Intestine	1.73 ± 0.48	0.21 ± 0.15	0.20 ± 0.10	0,20 ± 0,11	0.04 ± 0.00	0,03 ± 0,01
Adrenals	4.14 ± 1.46	0.71 ± 0.3	1.20 ± 0.12	0.72 ± 0.4	1.24 ± 0.16	0.46 ± 0.02

B. Peptide mass dependence of [^{111}In]-RM1 pharmacokinetics

Organ	10 pmol		50 pmol		100 pmol		250 pmol	
	4 h	24 h	4 h	24 h	4 h	24 h	4 h	24 h
Tumor	13.46 ± 0.80	6.58 ± 1.14	12.29 ± 2.68	3.92 ± 0.55	10.97 ± 0.99	4.66 ± 0.44	8.22 ± 0.93	4.41 ± 0.28
Pancreas	1.32 ± 0.31	0.15 ± 0.02	0.88 ± 0.13	0.10 ± 0.02	0.70 ± 0.12	0.11 ± 0.02	0.37 ± 0.11	0.08 ± 0.01
Stomach	0.76 ± 0.14	0.05 ± 0.02	0.49 ± 0.15	0.03 ± 0.01	0.51 ± 0.19	0.05 ± 0.02	0.21 ± 0.04	0.06 ± 0.00
Intestine	0.20 ± 0.12	0.04 ± 0.00	0.14 ± 0.03	0.04 ± 0.01	0.14 ± 0.03	0.04 ± 0.00	0.07 ± 0.01	0.05 ± 0.01
Adrenals	1.20 ± 0.12	1.24 ± 0.16	0.78 ± 0.18	0.57 ± 0.19	0.59 ± 0.11	0.49 ± 0.07	0.22 ± 0.07	0.41 ± 0.02

C. Biodistribution of [^{111}In]-RM1 under conditions where the GRPR were occupied by cold antagonist (2,000-fold)

Organ	1 h	4 h	24 h	1 h*
Tumor	4.47 ± 1.32	8.75 ± 0.47	11.79 ± 0.83	14.24 ± 1.75
Pancreas	2.79 ± 0.18	18.24 ± 2.00	21.21 ± 4.58	21.92 ± 1.34
Stomach	0.55 ± 0.03	2.90 ± 0.14	3.97 ± 0.75	3.31 ± 0.63
Intestine	0.40 ± 0.11	1.52 ± 0.34	1.63 ± 0.36	1.73 ± 0.48
Adrenals	0.65 ± 0.20	3.08 ± 1.29	2.64 ± 0.84	4.14 ± 1.46

NOTE: Displacement was done with 2,000-fold excess cold RM1. [^{111}In]-RM1 (0.18 MBq) was injected along with 10, 50, 100, and 250 pmol cold RM1. Animals were sacrificed at 4 and 24 h. Cold peptide (20 nmol) was injected first, followed by [^{111}In]-RM1 (5 μCi, 10 pmol) at 1, 4, and 24 h. Mice were sacrificed 1 h after [^{111}In]-RM1 injection.
Abbreviation: Displ, displacement.
*No preblocking with excess RM1.

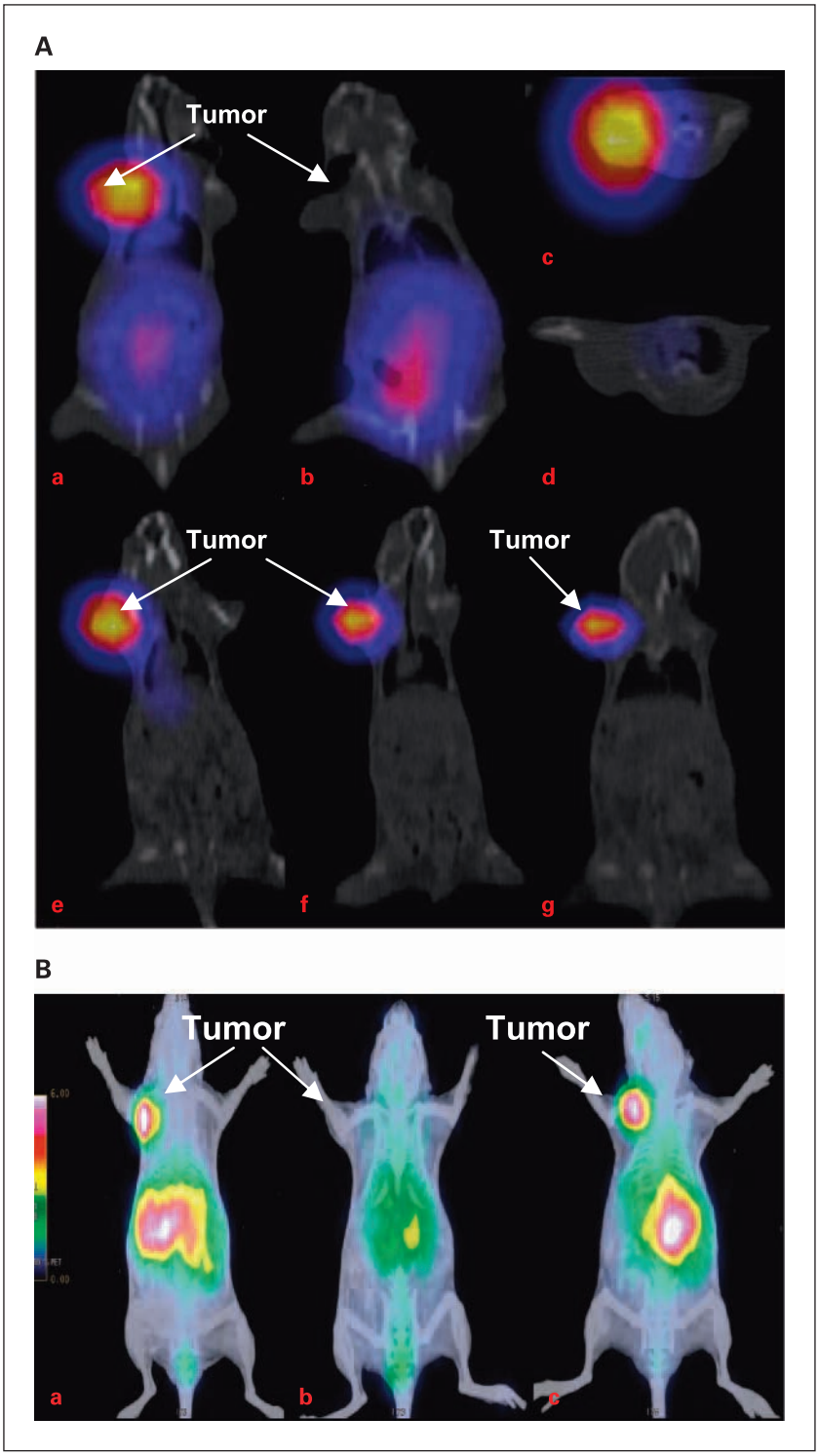

Fig. 4. *A,* SPECT/CT images of PC-3 tumor–bearing nude mice after injection of [^{111}In]-RM1 at 4 h (*a*), 4 h blocking (*b*), 24 h (*e*), 48 h (*f*), and 72 h (*g*). *c* and *d,* the transaxial SPECT/CT images at 4 and 4 h blocked, respectively. *B,* PET/CT images of PC-3 tumor–bearing nude mice after injection of [^{68}Ga]-RM1 at 1 h (*a*), 1 h blocking (*b*), and 2 h (*c*).

The images of [^{68}Ga]-RM1 PET/CT at 1 hour (blocked and unblocked) in Fig. 4B show the specificity of tracer uptake in the tumor and the abdominal receptor–positive organs.

Discussion

Bombesin-based radioagonists as targeting agents for prostate cancer have been described in preclinical (17-24) and clinical studies (25-27). The first recently published [^{99m}Tc]-labeled bombesin-based radioantagonist showed a 2- to 4-fold higher tumor uptake than the agonist (31). The present study describes a radiolabeled bombesin analogue with proven antagonistic properties potentially useful for imaging (SPECT, PET) and radionuclide therapy of GRPR-positive tumors. We compared its pharmacologic properties *in vitro* and biodistribution in the PC-3 mouse model with the potent agonist [$^{nat/111}$In]-AMBA. During the reviewing process of this article, a paper was published describing another COOH-terminal–modified bombesin-based peptide conjugated to DOTA (40). The

radiopeptide was not shown to have antagonistic properties but the tumor uptake was specific and reasonably high. The washout of abdominal organs was fast compared with common agonists.

We have recently shown for the somatostatin receptors 2 and 3 that antagonists may be superior to agonists as imaging and therapeutic agents. We hypothesized that this might also hold for other radiopeptides and thus result in a paradigm shift. Another aspect needs to be considered in developing bombesin-based radiopeptides for patient studies. Agonists of the bombesin family were shown to have mitogenic properties (12) and infusion or injection of agonists have shown side effects (41). Therefore antagonists were developed for anticancer therapies (13-16). Thus, for safety reasons, radioantagonists should be prepared.

The important message of this work is as follows:

The DOTA-gly-amino-benzoic acid modification and In(III)-metallation of RM1 did not alter the potent antagonist properties of peptide RM26 (32).

The pharmacokinetics of [^{111}In]-RM1 shows its high potential for visualizing GRPR-positive tumors at very early time points. This is due to the high initial tracer uptake and high tumor-to-blood and tumor-to-muscle ratios. The comparison with the potent agonist [^{111}In]-AMBA shows the superiority of the radioantagonist regarding the high tumor uptake and tumor-to-normal tissue ratio. Moreover, the tumor-to-kidney ratio is high. The fast washout of the radiopeptide from GRPR-positive organs, e.g., the pancreas, intestine, or stomach is remarkable. Radioagonists such as [^{111}In]-AMBA usually show very high uptake in these organs, especially in the pancreas. [^{111}In]-RM1 also shows a high initial pancreas uptake, but at 24 hours after injection, >99% of radioactivity is washed out, contrary to [^{111}In]-AMBA, which is retained in the pancreas most likely due to an effective internalization and cell retention. The tumor visualization using SPECT/CT supports these promising pharmacokinetic data. We cannot exclude at this moment that species differences are responsible for this somewhat surprising pharmacokinetic property as the PC-3 tumor is of human origin (42). If the pancreas washout were similarly fast in humans, this could be another important advantage of the radioantagonist as the high and persistent pancreas uptake of radioagonists in patients is very critical. These pharmacokinetic data leading to high tumor-to-normal tissue ratios already at early time points prompted us to study also the pharmacokinetics of [^{68}Ga]-RM1 as a new PET tracer.

[^{68}Ga]-RM1 showed similar pharmacokinetics to [^{111}In]-RM1 with lower kidney uptake and retention, a phenomenon known from Gallium- versus Indium-labeled DOTA-conjugated somatostatin-based octapeptides. These very promising pharmacokinetic and PET/CT imaging data render [^{68}Ga]-RM1 a future candidate for clinical GRPR-PET/CT studies. It may be superior to currently discussed [^{18}F]- and [^{64}Cu]-labeled agonists, which show high abdominal uptake and generally low tumor-to-normal tissue ratios (19–21, 43, 44). A distinct improvement of the tumor-to-intestine and tumor-to-kidney ratios was recently reported by Prasanphanich et al. (45) using the PET tracer [^{64}Cu-NOTA-8-Aoc]-BBN (7–14).

Two important questions concerning the present data remain to be answered. First, what causes the superior tumor uptake of the antagonist versus the agonist despite a 10-fold lower GRPR affinity? Second, why is the tumor washout relatively slow and unlike the one from pancreas and abdominal organs?

For the results on sst2/sst3, we assumed that antagonists detect more native receptors than agonists, a 75-fold higher receptor number was recognized for sst3 (6). These findings are consistent with the predictions of a model for G protein–coupled receptors in which an agonist binds to a receptor site with high affinity only to the fraction of receptors associated with the G protein, whereas the antagonist may additionally recognize uncoupled receptors (46).

For the agonist/antagonist pair studied here along with the human tumor–derived PC-3 cells *in vitro*, the radioantagonist showed a 3-fold higher B_{max}. This may explain the higher tumor uptake but we cannot exclude that *in vivo* receptor pharmacology is different to the *in vitro* situation.

We did different experiments to understand the long tumor retention. Agonists are well known to induce internalization of their receptors. This process usually removes the receptor-ligand complex from the plasma membrane and may highly depend on the ligand structure; however, as we have recently shown potent sst_2-receptor agonists may not induce receptor internalization (47). Most GPCRs remain at the cell surface upon antagonist binding but this cannot be generalized as CCK2 receptors were shown to internalize upon antagonist binding (48). Radioligand experiments, under conditions relevant to *in vivo* tumor targeting, showed efficient internalization of [^{111}In]-AMBA. Immunofluorescence-based internalization experiments confirm these results by showing high [^{nat}Lu]-AMBA–induced internalization rates.

A very low internalization of [^{111}In]-RM1 was shown in the radioligand internalization assay. Antagonists are able to bind in a multistep process by migration from a more peripheral to a central binding site. Therefore, we studied the time dependence of the replacement of [^{111}In]-RM1 from the receptor by injecting cold antagonists at different time points after [^{111}In]-RM1 injection. Our results suggest either *in vivo* internalization at a slow rate or, as mentioned above, slow migration of the radioantagonist from an accessible to a more central, inaccessible binding site.

Another experiment may shed light on the antagonist kinetics at the tumor cell surface and in the tumor compartment. We studied the [^{111}In]-RM1 uptake in GRPR-positive tissues and the tumor as a function of time under conditions where the receptors were presaturated by injection of a large excess of cold antagonist (RM1). At different time intervals, [^{111}In]-RM1 was injected and the animals sacrificed 1 hour later. The experiment was designed to determine the time point of receptor availability for radioligand binding compared with the control value set at 1 hour after injection. The results were different between tumor and abdominal organs. About half of the receptors were found to be available for radioligand binding at 4 hours, increasing to ~80% at 24 hours. These data apparently show a faster tumor washout of RM1 (in excess) compared with [^{111}In]-RM1. This difference may be explained by rebinding of the low-mass [^{111}In]-RM1 tracer.

Conclusion

Compared with the most potent DOTA-coupled agonist, [^{111}In]/[^{177}Lu]-AMBA, [^{111}In]-RM1, and [^{68}Ga]-RM1 show superior properties. These radiopeptides certainly deserve consideration regarding their development into clinically studied diagnostic agents to overcome shortcomings of agents like [^{18}F]-FDG or [^{11}C]choline in imaging and staging prostate cancer but may also be developed into therapeutic agents. Moreover, for the sake of potential toxicity, it may be advisable

and safer to develop radiolabeled antagonists for GRPR-positive tumor targeting.

Disclosure of Potential Conflicts of Interest

None of the authors disclosed potential conflicts of interest.

Acknowledgments

We thank Novartis Pharma for analytic assistance; Dr. M. Fani and Dr. A. Bauman for their support in Ga-68 labeling; S. Tschumi, E. Rauber, V. Rufener-Schirp, and M. Frischknecht for their expert technical help; and Bayer Schering Pharma for financial support.

References

1. Reubi JC. Peptide receptors as molecular targets for cancer diagnosis and therapy. Endocr Rev 2003;24:389–427.
2. Weiner RE, Thakur ML. Radiolabeled peptides in oncology: role in diagnosis and treatment. BioDrugs 2005;19:145–63.
3. Reubi JC, Maecke HR, Krenning EP. Candidates for peptide receptor radiotherapy today and in the future. J Nucl Med 2005;46:67–75S.
4. Heppeler A, Froidevaux S, Eberle AN, Maecke HR. Receptor targeting for tumor localisation and therapy with radiopeptides. Curr Med Chem 2000;7:971–94.
5. Boerman OC, Oyen WJ, Corstens FH. Radiolabeled receptor-binding peptides: a new class of radiopharmaceuticals. Semin Nucl Med 2000;30:195–208.
6. Ginj M, Zhang H, Waser B, et al. Radiolabeled somatostatin receptor antagonists are preferable to agonists for *in vivo* peptide receptor targeting of tumors. Proc Natl Acad Sci U S A 2006;103:16436–41.
7. Markwalder R, Reubi JC. Gastrin-releasing peptide receptors in the human prostate: relation to neoplastic transformation. Cancer Res 1999;59:1152–9.
8. Sun B, Halmos G, Schally AV, Wang X, Martinez M. Presence of receptors for bombesin/gastrin-releasing peptide and mRNA for three receptor subtypes in human prostate cancers. Prostate 2000;42:295–303.
9. Gugger M, Reubi JC. Gastrin-releasing peptide receptors in non-neoplastic and neoplastic human breast. Am J Pathol 1999;155:2067–76.
10. Halmos G, Wittliff JL, Schally AV. Characterization of bombesin/gastrin-releasing peptide receptors in human breast cancer and their relationship to steroid receptor expression. Cancer Res 1995; 55:280–7.
11. Reubi JC, Korner M, Waser B, Mazzucchelli L, Guillou L. High expression of peptide receptors as a novel target in gastrointestinal stromal tumours. Eur J Nucl Med Mol Imaging 2004;31: 803–10.
12. Cuttitta F, Carney DN, Mulshine J, et al. Bombesin-like peptides can function as autocrine growth factors in human small-cell lung cancer. Nature 1985;316:823–6.
13. Cornelio DB, Roesler R, Schwartsmann G. Gastrin-releasing peptide receptor as a molecular target in experimental anticancer therapy. Ann Oncol 2007;18:1457–66.
14. Stangelberger A, Schally AV, Varga JL, et al. Inhibitory effect of antagonists of bombesin and growth hormone-releasing hormone on orthotopic and intraosseous growth and invasiveness of PC-3 human prostate cancer in nude mice. Clin Cancer Res 2005;11:49–57.
15. Bajo AM, Schally AV, Groot K, Szepeshazi K. Bombesin antagonists inhibit proangiogenic factors in human experimental breast cancers. Br J Cancer 2004;90:245–52.
16. Schwartsmann G, DiLeone LP, Horowitz M, et al. A phase I trial of the bombesin/gastrin-releasing peptide (BN/GRP) antagonist RC3095 in patients with advanced solid malignancies. Invest New Drugs 2006;24:403–12.
17. Nock BA, Nikolopoulou A, Galanis A, et al. Potent bombesin-like peptides for GRP-receptor targeting of tumors with ^{99m}Tc: a preclinical study. J Med Chem 2005;48:100–10.
18. Lantry LE, Cappelletti E, Maddalena ME, et al. ^{177}Lu-AMBA: synthesis and characterization of a selective ^{177}Lu-labeled GRP-R agonist for systemic radiotherapy of prostate cancer. J Nucl Med 2006;47:1144–52.
19. Chen X, Park R, Hou Y, et al. microPET and autoradiographic imaging of GRP receptor expression with ^{64}Cu-DOTA-[Lys^3]bombesin in human prostate adenocarcinoma xenografts. J Nucl Med 2004;45:1390–7.
20. Zhang X, Cai W, Cao F, et al. ^{18}F-labeled bombesin analogs for targeting GRP receptor-expressing prostate cancer. J Nucl Med 2006;47:492–501.
21. Lin KS, Luu A, Baidoo KE, et al. A new high affinity technetium-99m-bombesin analogue with low abdominal accumulation. Bioconjug Chem 2005;16:43–50.
22. Schuhmacher J, Zhang H, Doll J, et al. GRP receptor-targeted PET of a rat pancreas carcinoma xenograft in nude mice with a ^{68}Ga-labeled bombesin(6-14) analog. J Nucl Med 2005;46:691–9.
23. Parry JJ, Andrews R, Rogers BE MicroPET Imaging of Breast Cancer Using Radiolabeled Bombesin Analogs Targeting the Gastrin-releasing Peptide Receptor. Breast Cancer Res Treat 2006; 2007;101:175–183.
24. Zhang H, Chen J, Waldherr C, et al. Synthesis and evaluation of bombesin derivatives on the basis of pan-bombesin peptides labeled with indium-111, lutetium-177, and yttrium-90 for targeting bombesin receptor-expressing tumors. Cancer Res 2004;64:6707–15.
25. Van de Wiele C, Dumont F, Vanden Broecke R, et al. Technetium-99m RP527, a GRP analogue for visualisation of GRP receptor-expressing malignancies: a feasibility study. Eur J Nucl Med 2000;27:1694–9.
26. Van de Wiele C, Phonteyne P, Pauwels P, et al. Gastrin-releasing peptide receptor imaging in human breast carcinoma versus immunohistochemistry. J Nucl Med 2008;49:260–4.
27. Dimitrakopoulou-Strauss A, Hohenberger P, Haberkorn U, Maecke HR, Eisenhut M, Strauss LG. ^{68}Ga-labeled bombesin studies in patients with gastrointestinal stromal tumors: comparison with ^{18}F-FDG. J Nucl Med 2007;48:1245–50.
28. Bodei L, Ferrari M, Nunn AD, et al. 177Lu-AMBA Bombesin analogue in hormone refractory prostate cancer patients: a phase I escalation study with single-cycle administrations. Eur J Nucl Med Mol Imaging 2007;34:S221.
29. Baum RP, Prasad V, Mutloka N, Frischknecht M, Maecke HR, Reubi JC. Molecular imaging of bombesin receptors in various tumors by Ga-68 AMBA PET/CT. J Nucl Med 2007;48:79P.
30. Azay J, Nagain C, Llinares M, et al. Comparative study of *in vitro* and *in vivo* activities of bombesin pseudopeptide analogs modified on the C-terminal dipeptide fragment. Peptides 1998;19:57–63.
31. Cescato R, Maina T, Nock B, et al. Bombesin receptor antagonists may be preferable to agonists for tumor targeting. J Nucl Med 2008;49:318–26.
32. Llinares M, Devin C, Chaloin O, et al. Syntheses and biological activities of potent bombesin receptor antagonists. J Pept Res 1999;53:275–83.
33. Atherton E, Sheppard R. Fluorenylmethoxycarbonyl-polyamide solid phase peptide synthesis. General principles and development. Oxford: Oxford Information Press; 1989.
34. Heppeler A, Froidevaux S, Mäcke H, et al. Radiometal-labelled macrocyclic chelator-derivatised somatostatin analogue with superb tumour-targeting properties and potential for receptor-mediated internal radiotherapy. Chemistry 1999; 5:1974–81.
35. Zhernosekov KP, Filosofov DV, Baum RP, et al. Processing of generator-produced ^{68}Ga for medical application. J Nucl Med 2007;48:1741–8.
36. Reubi JC, Wenger S, Schmuckli-Maurer J, Schaer JC, Gugger M. Bombesin receptor subtypes in human cancers: detection with the universal radioligand ^{125}I-[D-TYR^6, β-ALA^{11}, PHE^{13}, NLE^{14}] Bombesin(6–14). Clin Cancer Res 2002; 8:1139–46.
37. Vigna SR, Mantyh CR, Giraud AS, Soll AH, Walsh JH, Mantyh PW. Localization of specific binding sites for bombesin in the canine gastrointestinal tract. Gastroenterology 1987;93: 1287–95.
38. Michel N, Ganter K, Venzke S, Bitzegeio J, Fackler OT, Keppler OT. The Nef protein of human immunodeficiency virus is a broad-spectrum modulator of chemokine receptor cell surface levels that acts independently of classical motifs for receptor endocytosis and Gαi signaling. Mol Biol Cell 2006;17:3578–90.
39. Fox J, Maddalena M, Wedeking P, et al. Comparative biodistributions of ^{111}In, ^{67}Ga and ^{177}Lu-AMBA in PC-3 tumor bearing mice. J Nucl Med 2007;48:79P.
40. Abd-Elgaliel WR, Gallazzi F, Garrison JC, et al. Design, synthesis, and biological evaluation of an antagonist-bombesin analogue as targeting vector. Bioconjug Chem 2008;19:2040–8.
41. Basso N, Lezoche E, Speranza V. Studies with bombesin in man. World J Surg 1979;3:579–85.
42. Maina T, Nock BA, Zhang H, et al. Species differences of bombesin analog interactions with GRP-R define the choice of animal models in the development of GRP-R-targeting drugs. J Nucl Med 2005;46:823–30.
43. Yang Y-S, Zhang X, Xiong Z, Chen X. Comparative *in vitro* and *in vivo* evaluation of two ^{64}Cu-labeled bombesin analogs in a mouse model of human prostate adenocarcinoma. Nucl Med Biol 2006;33:371–80.
44. Rogers BE, Bigott HM, McCarthy DW, et al. MicroPET Imaging of a gastrin-releasing peptide receptor-positive tumor in a mouse model of human prostate cancer using a ^{64}Cu-labeled bombesin analogue. Bioconjug Chem 2003;14: 756–63.
45. Prasanphanich AF, Nanda PK, Rold TL, et al. [^{64}Cu-NOTA-8-Aoc-BBN(7–14)NH$_2$] targeting vector for positron-emission tomography imaging of gastrin-releasing peptide receptor-expressing tissues. Proc Natl Acad Sci U S A 2007;104:12462–7.
46. Kenakin T. New concepts in drug discovery: collateral efficacy and permissive antagonism. Nat Rev Drug Discov 2005;4:919–27.
47. Ginj M, Zhang H, Eisenwiener KP, et al. New pansomatostatin ligands and their chelated versions: affinity profile, agonist activity, internalization, and tumor targeting. Clin Cancer Res 2008;14:2019–27.
48. Roettger BF, Ghanekar D, Rao R, et al. Antagonist-stimulated internalization of the G protein-coupled cholecystokinin receptor. Mol Pharmacol 1997;51:357–62.